CHAPTER 7
POLARIZATION-SENSITIVE MULTIPATH PROPAGATION MODELING

7.1 Introduction

A variety of propagation models have been reported in the literature that approximate characteristics of a radio channel, including path loss, shadowing, and multipath effects. These models provide some insight into the effects of different channel characteristics on wireless communication systems. Models can be used for preliminary evaluation of system alternatives before investing in prototype hardware.

Current propagation models do not consider the polarization of transmitted signal, depolarization introduced by the channel, or polarized multipath. Propagation models that include polarization effects will be useful for evaluating the performance of polarization-sensitive adaptive arrays and diversity reception techniques. While polarization-sensitive adaptive arrays have been proposed as described in Chapter 5, their performance has not been evaluated in multipath channels. In this chapter, existing multipath propagation models are extended to include the effects of antenna pattern, antenna orientation, and wave polarization.

7.2 Existing Multipath Propagation Models

Many multipath propagation models have been developed for evaluating antenna diversity and adaptive array systems. Several of these models are summarized in [7.1]. These models typically assume there are a number of objects that cause scattering or specular reflections (for brevity both of these will be referred to as "scatterers") in the vicinity of the transmitter and/or receiver. The signal at the receiver consists of signals reflected or scattered from objects, and possibly also a line-of-sight component. These models generate several multipath components, each having distinct amplitude, phase, and angle of arrival at each receiving antenna. The models yield a vector containing the resultant signal at each antenna due to all the multipath components. Because of this, these models are sometimes called vector channel models.

Site-specific propagation prediction approaches such as ray tracing and finite-difference time domain (FDTD) are deterministic and exploit knowledge of physical objects in the propagation environment and their properties. These models can provide

good agreement with measured results [7.2], but detailed information on the size, shape, and location of objects in the channel is required. In addition, extensive measurements are required to optimize such models for a specific location.

In contrast, more general models like those described in this section address channels with specific characteristics (i.e. multipath delay and angle spread) but do not attempt to represent a specific channel exactly. The models discussed here include free-space path loss and are useful for simulating multipath effects but do not attempt to simulate the effects of shadowing. These models can be deterministic, with scatterers placed in specific locations, as in Lee's model, or stochastic like Liberti's and Petrus' models, where scatterers are distributed randomly. Deterministic simulations can be performed using a specific sample of scatterers from the Petrus or Liberti models, but the scatterer locations are not chosen to simulate a particular physical channel as they are in site-specific models.

Propagation conditions in a wireless communication system vary depending on the position of the mobile or hand-held unit. The line-of-sight path is obstructed in some cases but not others. The channel models described in this chapter represent a "worst case" where several multipath components have similar power levels. In this scenario very deep fades occur. These models require much less information and computation than site-specific models such as ray tracing and FDTD, and are useful for assessing the performance of a system in a range of channel conditions. Three general vector channel models are discussed below.

7.2.1 Ring of scatterers model (Lee)

Lee's model [7.3] assumes that the base station antenna is located above the terrain and buildings, as in a macrocell system, so that reflections occur near the mobile and not near the base station. In this model, scatterers are evenly spaced on a circle about the mobile as shown in Fig. 7-1. The radius of the ring of scatterers is 30-60 m or about 100-200 wavelengths at 850 MHz. The contribution of the reflected ray from each scatterer at the receiver is calculated. Several variations on this model are discussed in [7.1].

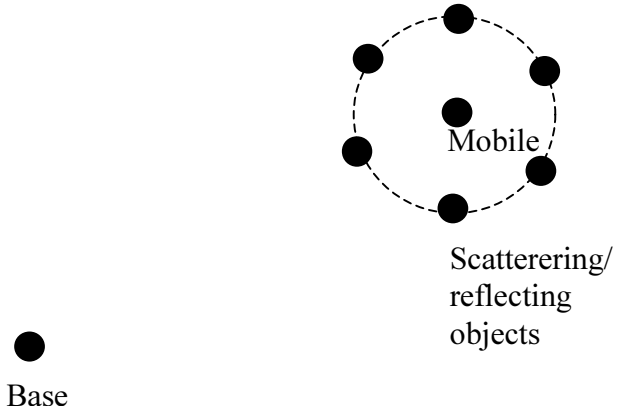

Figure 7-1. Ring of scatterers model (Lee)

7.2.2 Geometrically-based single-bounce circular model (Petrus)

Another model that represents a macrocell environment is the geometrically-based single-bounce circular model [7.4]. This model places a selected number of scatterers randomly with a uniform probability distribution within a circular region surrounding the mobile, as in Fig. 7-2. From there, modeling proceeds as in Lee's model.

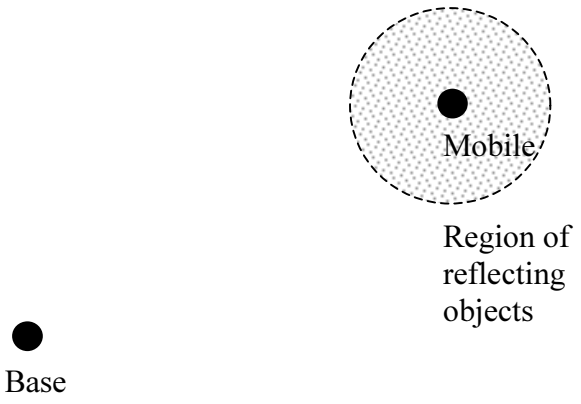

Figure 7-2. Geometrically-based single-bounce circular model

7.2.3 Geometrically-based single-bounce elliptical model (Liberti)

The geometrically based single-bounce elliptical model [7.5] represents a microcell scenario in which the base and mobile antennas are both located below the tops of surrounding building and terrain. Single-bounce reflections that arrive with a given

delay are due to reflecting objects that lie on an ellipse that has its foci at the base and mobile locations. In this model, reflectors are randomly located with a uniform probability distribution within a region bounded by the ellipse that corresponds to the maximum delay in the channel. Figure 7-3 shows this region of scatterers.

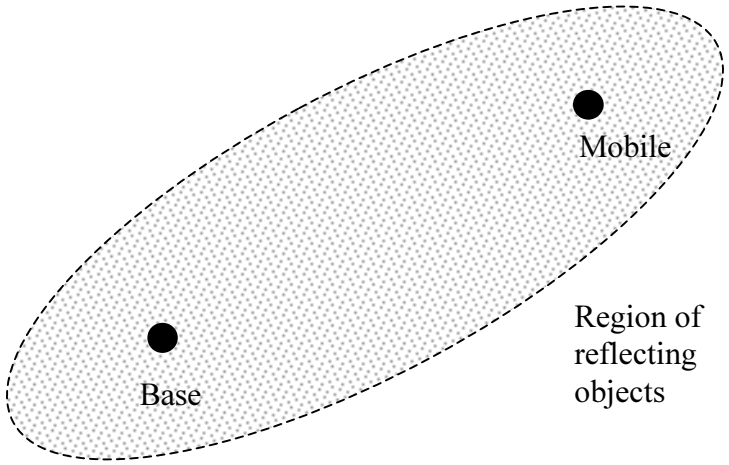

Figure 7-3. Geometrically-based single-bounce elliptical model

7.3 Reflection of Polarized Waves

The reflection of a polarized wave at a planar surface depends on the properties of the material and on the angle of incidence and polarization of the incoming wave. Because orthogonally polarized components of the wave are reflected differently, reflection usually results in some depolarization of the wave.

The Fresnel reflection coefficients [7.6] describe the reflection of polarized waves at the planar interface of two dissimilar media, as shown in Fig. 7-4. The Fresnel coefficients are based on the assumptions that the media and their interface are infinite in extent, and that the interface is smooth. This is approximately true if irregularities in the interface are much smaller than a wavelength, and the dimensions of the interface and the depth of the media are much larger than a wavelength.

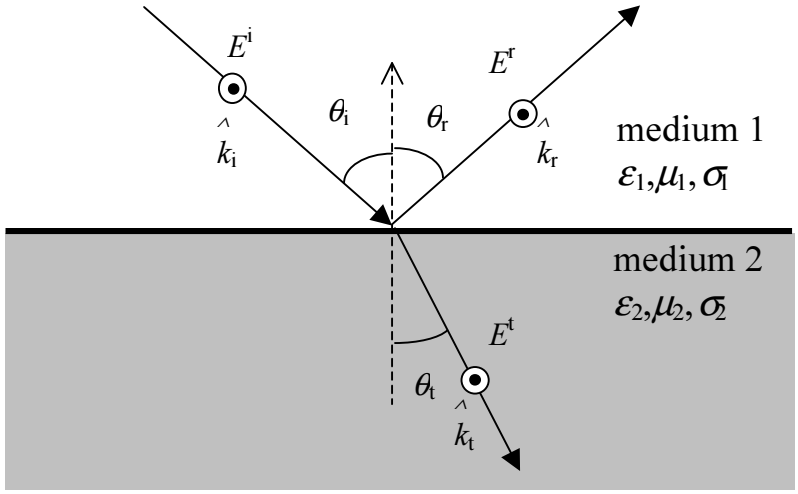

Figure 7-4. Reflection and transmission of polarized wave (perpendicular polarization shown)

The Fresnel reflection coefficients for polarizations perpendicular and parallel to the plane of incidence are as follows.

$$\Gamma_{\parallel} = \frac{E_{\parallel}^r}{E_{\parallel}^i} = \frac{-\eta_1 \cos\theta_i + \eta_2 \cos\theta_t}{\eta_1 \cos\theta_i + \eta_2 \cos\theta_t} \tag{7.1}$$

$$\Gamma_{\perp} = \frac{E_{\perp}^r}{E_{\perp}^i} = \frac{\eta_2 \cos\theta_i - \eta_1 \cos\theta_t}{\eta_2 \cos\theta_i + \eta_1 \cos\theta_t} \tag{7.2}$$

where

$$\theta_r = \theta_i$$

$$k_1 \sin\theta_i = k_2 \sin\theta_t$$

$$\eta = \sqrt{\frac{\mu}{\varepsilon}}$$

$$k = \omega\sqrt{\mu\varepsilon}$$

The Fresnel coefficients provide accurate reflection information if the previous assumptions are valid, and represent the polarization-sensitive nature of wave reflection. In practice, the assumptions often do not hold. In addition, the computation involved in this rigorous approach to modeling reflections may not be justified in a general

propagation model. An alternative is to use reflection coefficients that do not include dependence on the angle of incidence. This introduces an approximation but requires less computation. Constant reflection coefficients can be assumed to be the same or different for different polarizations, and can be determined based on the mean of the Fresnel coefficients or based on some empirical approach, as is often the case in ray-tracing models. Reflection using constant reflection coefficients will introduce some depolarization unless the transmitted wave has pure vertical or pure horizontal polarization.

7.4 Geometric Components for Modeling Transmission and Reception of Polarized Waves in a Mobile Communication System

To evaluate the performance of polarization diversity or polarization-sensitive adaptive array systems, it is necessary to model the propagation environment and the antenna patterns in a way that includes polarization information. Mobile radios generally use vertically polarized antennas. Handsets typically use linearly polarized antennas, but the orientation of the antenna is random. When the handset is held to the user's ear, the antenna is inclined approximately 60° from vertical, and the azimuth angle is random with a uniform probability distribution, if the user is assumed to be equally likely to face any direction.

It is useful to represent electric field antenna patterns in terms of vertical and horizontal components for any antenna orientation. This section presents a three-dimensional representation of the antenna pattern and procedures for rotating the pattern and determining the vertical and horizontal components of the rotated pattern.

Modeling the reception of polarized waves in a multipath channel leads to a new definition of polarization for multipath signals. This can be used to generate fading envelopes for diversity systems or spatial-polarization signatures for adaptive arrays.

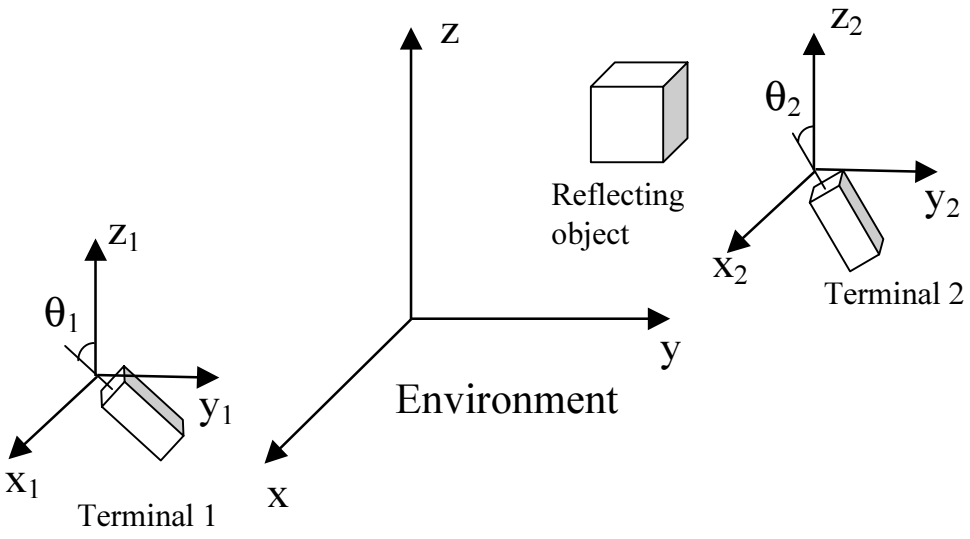

Figure 7-5. Coordinate systems for modeling transmission and reception of polarized waves

7.4.1 Antenna pattern representation for polarization-sensitive channel modeling

To facilitate polarization-sensitive channel modeling, antenna patterns are represented in three dimensions. Vertical and horizontal electric field component patterns are sampled at regularly spaced angles θ and ϕ. This has been implemented in MATLAB with the sampling resolution specified in degrees. Resolutions must be chosen so that the angles at which the pattern is sampled include θ=90° and ϕ=360°. A typical sampled pattern is shown in Fig. 7-6. Note that in this particular case the antenna is a purely vertically polarized half-wave dipole so the pattern has no horizontally polarized component.

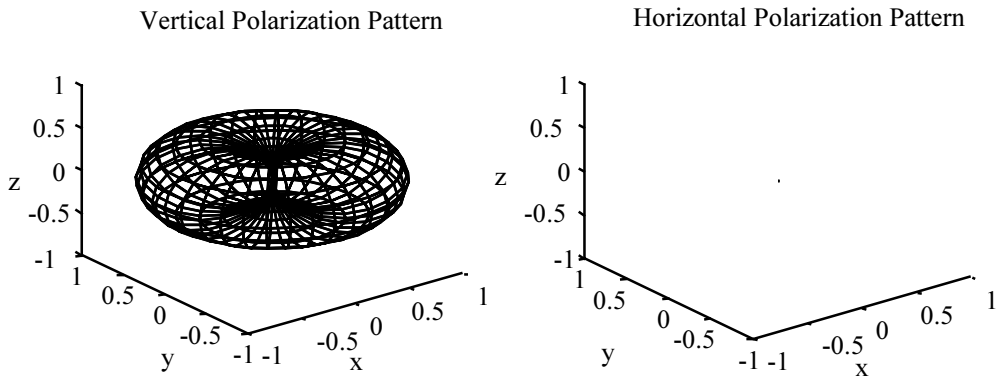

Figure 7-6. Sampled 3-dimensional pattern of a vertical half-wave dipole with 10° resolution in θ and ϕ. The pattern has no horizontally polarized component.

7.4.2 Antenna pattern rotation and resampling [7.7]

A procedure was developed [7.7] to represent the pattern of an antenna that has been rotated. This procedure is shown graphically in Fig. 7-7.

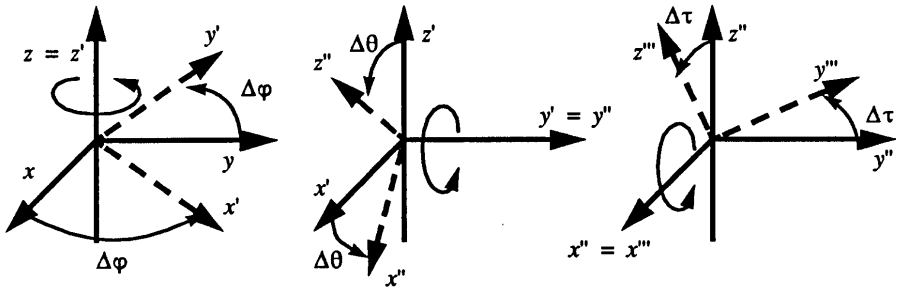

Figure 7-7. A three step rotation procedure that provides the ability to point the antenna in an arbitrary direction. The rotated pattern is referred back to the original coordinate system [7.7]

In the rotation procedure, the complex value of the antenna pattern sampled at point $P_c = [x \quad y \quad z]^T$ becomes the value of the rotated pattern at the new point $P_{c,3} = [x_3 \quad y_3 \quad z_3]^T$. The new point is obtained by a transformation as follows.

$$P_{c,3} = R_1 R_2 R_3 P_c \tag{7.3}$$

R_1, R_2, and R_3 are transformation matrices for the three rotations shown in Fig. 7-7.

The transformation matrices are

$$R_1 = \begin{bmatrix} \cos\Delta\phi & -\sin\Delta\phi & 0 \\ \sin\Delta\phi & \cos\Delta\phi & 0 \\ 0 & 0 & 1 \end{bmatrix} \tag{7.4}$$

$$R_2 = \begin{bmatrix} \cos\Delta\theta & 0 & \sin\Delta\theta \\ 0 & 1 & 0 \\ -\sin\Delta\theta & 0 & \cos\Delta\theta \end{bmatrix} \tag{7.5}$$

$$R_3 = \begin{bmatrix} 1 & 0 & 0 \\ 0 & \cos\Delta\tau & -\sin\Delta\tau \\ 0 & \sin\Delta\tau & \cos\Delta\tau \end{bmatrix} \tag{7.6}$$

In spherical coordinates, the sampling points are $P_c = (1, \theta, \phi)$ (before rotation) and $P_{c,3} = (1, \theta''', \phi''')$ where the triple prime denotes the three rotations ($\Delta\phi$,$\Delta\theta$, and $\Delta\tau$). The original vertically and horizontally polarized patterns are rotated to obtain

$$\begin{aligned} f_{V,rot}(P_{c,3}) &= f_{V,rot}(\theta''', \phi''') = f_V(P_c) = f_V(\theta, \phi) \\ f_{H,rot}(P_{c,3}) &= f_{H,rot}(\theta''', \phi''') = f_H(P_c) = f_H(\theta, \phi) \end{aligned} \tag{7.7}$$

The rotated patterns are then resampled at the nearest discrete points (θ, ϕ) determined by the sampling resolution. The relationships between spherical and rectangular coordinates are given by

$$\begin{aligned} r &= \sqrt{x^2 + y^2 + z^2} \\ \theta &= \tan^{-1}\left(\frac{\sqrt{x^2 + y^2}}{z} \right) \\ \phi &= \tan^{-1}\left(\frac{y}{x} \right) \end{aligned} \tag{7.8}$$

and

$$\begin{aligned} x &= r\sin\theta\cos\phi \\ y &= r\sin\theta\sin\phi \\ z &= r\cos\theta \end{aligned} \tag{7.9}$$

7.4.3 Antenna pattern repolarization

The pattern samples $f_{V,rot}(P_{c3})$ and $f_{H,rot}(P_{c3})$ obtained after rotating the pattern no longer represent vertical and horizontal polarizations. It is relatively straightforward to obtain the new vertically and horizontally polarized components of the rotated pattern, and the procedure is described below. This procedure corresponds to Ludwig's second definition of cross polarization [7.8] and is also compatible with patterns obtained from measurements using an azimuth-over-elevation positioner or from moment-method codes such as NEC and WIRE.

All vectors shown in this procedure are represented in terms of the original basis vectors $\hat{x} = [1 \quad 0 \quad 0]^T$, $\hat{y} = [0 \quad 1 \quad 0]^T$, and $\hat{z} = [0 \quad 0 \quad 1]^T$.

For a point P_c=(1,θ, ϕ) the unit vectors are given by

$$\hat{r} = [\sin\theta\cos\phi \quad \sin\theta\sin\phi \quad \cos\theta] \tag{7.10a}$$

$$\hat{\phi} = \frac{\hat{z}\times\hat{r}}{|\hat{z}\times\hat{r}|} \tag{7.10b}$$

$$\hat{\theta} = \frac{\hat{\phi}\times\hat{r}}{|\hat{\phi}\times\hat{r}|} \tag{7.10c}$$

After rotation the new rectangular unit vectors are $\hat{x}''' = R_1R_2R_3\hat{x}$, $\hat{y}''' = R_1R_2R_3\hat{y}$, and $\hat{z}''' = R_1R_2R_3\hat{z}$, where the triple prime denotes three rotations. The unit vector $\hat{r}$ is as defined in (7.10a) above, and the other spherical unit vectors are

$$\hat{\phi}''' = \frac{\hat{z}'''\times\hat{r}}{|\hat{z}'''\times\hat{r}|} \tag{7.11a}$$

$$\hat{\theta}''' = \frac{\hat{\phi}'''\times\hat{r}}{|\hat{\phi}'''\times\hat{r}|} \tag{7.11b}$$

The vertically polarized component of the rotated pattern (the component in the $\hat{\theta}$ direction) and the horizontally polarized component (the component in the $\hat{\phi}$ direction) are given by

$$f_{rot,V}(\theta,\phi) = [\hat{\theta}'''\cdot\hat{\theta}]f_{V,rot}(\theta,\phi) + [\hat{\phi}'''\cdot\hat{\theta}]f_{H,rot}(\theta,\phi) \tag{7.12a}$$

$$f_{rot,H}(\theta,\phi) = [\hat{\theta}''' \cdot \hat{\phi}] f_{V,rot}(\theta,\phi) + [\hat{\phi}''' \cdot \hat{\phi}] f_{H,rot}(\theta,\phi) \quad (7.12b)$$

The pattern of a half-wave dipole rotated by $\Delta\theta=20°$ from vertical is shown in Fig. 7-8

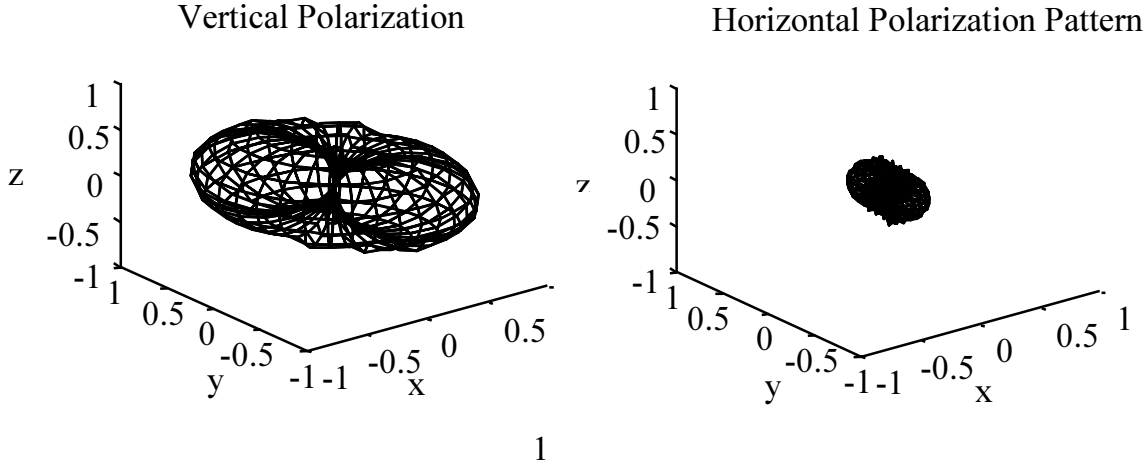

Figure 7-8. Pattern of a half-wave dipole that has been rotated by 20° from vertical

7.4.4 Gain of an arbitrarily polarized antenna

If dissimilar antenna elements are included in the same array or diversity combining system, it is necessary to know the element gain in order to model performance correctly. The gain of an antenna is given by

$$G=eD \quad (7.13)$$

where D is the directivity and e is the efficiency of the antenna. The directivity is defined as [7.9]

$$D=4\pi/\Omega_A \quad (7.14)$$

where the beam solid angle is given by

$$\Omega_A = \int_0^{2\pi}\int_0^{\pi} \left| f(\theta,\phi) \right|^2 \sin\theta d\theta d\phi \quad (7.15)$$

The power pattern can be represented in terms of horizontally and vertically polarized components as

$$|f(\theta,\phi)|^2=|f_H(\theta,\phi)|^2+|f_V(\theta,\phi)|^2 \quad (7.16)$$

The patterns can be normalized so that the pattern maximum corresponds to the maximum gain of the antenna, or

$$|f_N(\theta_{\max},\phi_{\max})|^2=G \quad (7.17)$$

This yields

$$f_N(\theta,\phi) = \frac{\sqrt{G}}{\left|f(\theta_{\max},\phi_{\max})\right|} f(\theta,\phi) \tag{7.18}$$

If the antenna does not have pure polarization, then

$$f_{H,N}(\theta,\phi) = \frac{\sqrt{G}}{\left|f(\theta_{\max},\phi_{\max})\right|} f_H(\theta,\phi) \tag{7.19a}$$

$$f_{V,N}(\theta,\phi) = \frac{\sqrt{G}}{\left|f(\theta_{\max},\phi_{\max})\right|} f_V(\theta,\phi) \tag{7.19b}$$

Note that after the rotation procedure described in Sections 7.4.2 and 7.4.3, the gain will be unchanged except for the error introduced by resampling the rotated pattern.

7.4.5 Polarization in Multipath Channels

Polarization states are well defined for plane waves. Because mobile radio channels typically include multipath propagation, a new definition is needed for these channels. Here three increasingly general definitions are presented that are applicable to multipath channels.

The horizontally and vertically polarized components of a plane wave are represented in phasor notation as follows [7.10]:

$$E_H = E_1 \tag{7.20a}$$

$$E_V = E_2 e^{j\delta} \tag{7.20b}$$

where E_1 and E_2 are the amplitudes of the horizontal and vertical components, respectively and δ is the phase of the vertically polarized part of the signal relative to the horizontally polarized part. The absolute phase is omitted. This definition does not apply in a multipath channel. The received signal in a multipath channel can be represented as the superposition of M plane waves. In general, each of these plane waves can have a different absolute phase, angle of arrival, and polarization state.

The following representation is independent of antenna pattern (or assumes isotropic horizontally and vertically polarized patterns):

$$E_H = \sum_{i=1}^{M} E_{1_i} e^{j\delta_i''} \tag{7.21a}$$

$$E_V = \sum_{i=1}^{M} E_{2_i} e^{j(\delta_i'' + \delta_i)} \tag{7.21b}$$

E_{1i} and E_{2i} are the horizontal and vertical components of the i^{th} plane wave, respectively and δ_i is the phase of the vertically polarized part of the i^{th} multipath component relative to the horizontally polarized part.

If a receiver uses two antennas that are oriented vertically and horizontally, the polarization can be defined in terms of the antenna response $g(\theta, \phi, P)$ as:

$$E_H = \sum_{i=1}^{M} g(\theta_i, \phi_i, H) E_{1_i} e^{j\delta_i''} \tag{7.22a}$$

$$E_V = \sum_{i=1}^{M} g(\theta_i, \phi_i, V) E_{2_i} e^{j(\delta_i'' + \delta_i)} \tag{7.22b}$$

In the general case of three dimensions, up to three orthogonal polarizations are possible. The polarization can be defined in terms of three polarizations as follows. In this case the polarizations are not assumed to be horizontal and vertical.

$$E'_{P_1} = \sum_{i=1}^{M} g(\theta_i, \phi_i, P_1) E_{1_i} e^{j\delta_i''} \tag{7.23a}$$

$$E'_{P_2} = \sum_{i=1}^{M} g(\theta_i, \phi_i, P_2) E_{2_i} e^{j(\delta_i'' + \delta_{2i})} \tag{7.23b}$$

$$E'_{P_3} = \sum_{i=1}^{M} g(\theta_i, \phi_i, P_3) E_{3_i} e^{j(\delta_i'' + \delta_{3i})} \tag{7.23c}$$

7.5 Simulation of Polarization-Sensitive Multipath Propagation [7.11]

The Vector Multipath Propagation Simulator (VMPS) was developed to function in conjunction with experimental measurements in either narrowband or wideband signal environments. The complete radio channel can be modeled with this simulator including antenna and propagation effects. Polarization is included in the models. The modeled results can be used to confirm experimental results and visa versa. The goal is to study and isolate the independent effects of such parameters as antenna pattern, polarization, and spacing, multipath, interference, algorithm performance, and others. This section draws extensively from a previous report on VMPS [7.11] but contains some additional material.

7.5.1 Description of VMPS

The vector multipath propagation simulator (VMPS) is a two-dimensional polarization-sensitive vector multipath channel modeling software tool that implements many of the features described in this chapter. A receiver system with up to 8 antennas can be modeled with the VMPS simulator. Up to 6 transmitters can be activated and placed at arbitrary locations around the receiver. Any of these transmitters can be selected to be the desired transmitter leaving the remaining activated transmitters as sources of interference. Multipath is simulated through the addition of scatterers in the propagation environment. The locations of scatterers seen by each transmitter are determined using built in multipath models can be selected by the user. Manual placement of scatterers is currently implemented for wideband simulations and will be supported for narrowband simulations in future versions of VMPS. The power sent out of each transmitter can be varied as well as two angle-independent reflection coefficients (one each for vertically and horizontally polarized waves) that apply to all of the scatterers associated with that transmitter. Additionally, the direct line of sight between the receiver and a given transmitter can be turned off or on, simulating blocked or unblocked line of sight. The combination of all these features allows for the simulation of a wide variety of channel conditions.

VMPS includes both wideband and narrowband modeling. The narrowband simulator can model the performance of receiving array configurations that include spatial, polarization, and pattern or angle diversity. Performance of array configurations with diversity combining as well as adaptive beamforming algorithms can be evaluated using VMPS. The result is to establish the statistics of diversity gain or interference rejection as a function of envelope correlation, multipath scenario, and antenna configuration. The diversity gain can be established for one of the following combining schemes: maximal ratio, selection, or equal gain combining. The diversity schemes are applied to the received signal envelopes at the antenna elements of a moving receiver within the propagation environment. A plot of the statistics of diversity gain and the individual envelopes received at the antennas can be plotted for a user-defined environment.

7.5.2 Simulation procedure

To simulate the performance of an adaptive array or diversity combining system the procedure shown below is used:

1. Generate antenna pattern files for transmitting and receiving antenna elements
2. Generate array pattern file for transmitting terminal (if array is used at transmitter)
3. Specify terminal locations, multipath model parameters
4. Calculate spatial signature of desired and interfering signals
5. Generate received signal(s) if needed
6. Apply adaptive or diversity combining algorithm
7. Compare SNR or SINR before and after combining

The terminal locations are specified for each simulation and the scatterer locations are determined using one of the models described in Section 7.2. The angles ϕ_0, ϕ_{1i}, and ϕ_{2i} are obtained directly from the system geometry, and the reflection angle ϕ_{ri} can be obtained from the other angles. From the system geometry and specification of the antennas at each terminal, a spatial signature and/or instantaneous received signal envelope can be obtained. By running consecutive simulations with one of the terminals moving, time-varying spatial signatures or spatial-polarization signatures (described in Chapter 3) and received signal envelopes can be obtained. These in turn can be used to evaluate the performance of adaptive and diversity combining systems.

As with the receiver, the transmitter can be given an arbitrary antenna pattern. In order to introduce multipath, scatterers (reflectors) can be introduced into to propagation environment. A multipath component arrives from each scatterer location which can be placed anywhere within the region. One of the built-in propagation models (Lee, Petrus, Liberti) can also be used to randomly place scatterers within the environment (see appendix). The number of scatterers as well as their reflection coefficients can be varied.

The version of VMPS used in this investigation represented used fixed scattering coefficients and retained the same scatterer locations as the receiver or transmitter moved. A newer version of VMPS that is currently being tested models specular reflection implemented such that the initial reflection is assumed to occur at a point on a planar surface. In the newer version of VMPS, the reflection point moves along the

surface as the receivers and/or transmitters moved so that the angles of incidence and reflection are kept equal.

The received signal at each antenna is the sum of all signals arriving at the antenna and the signal at each element can be combined using selection, equal gain, or maximal ratio combining. A series of programs has been developed for simulating polarization-sensitive multipath propagation. This software accounts for array geometry, antenna gain, pattern, orientation, and polarization at the transmitting and receiving terminals, and the multipath propagation environment. The simulation software allows for arbitrary location of the two terminals. An example geometry shown in Fig. 7-9

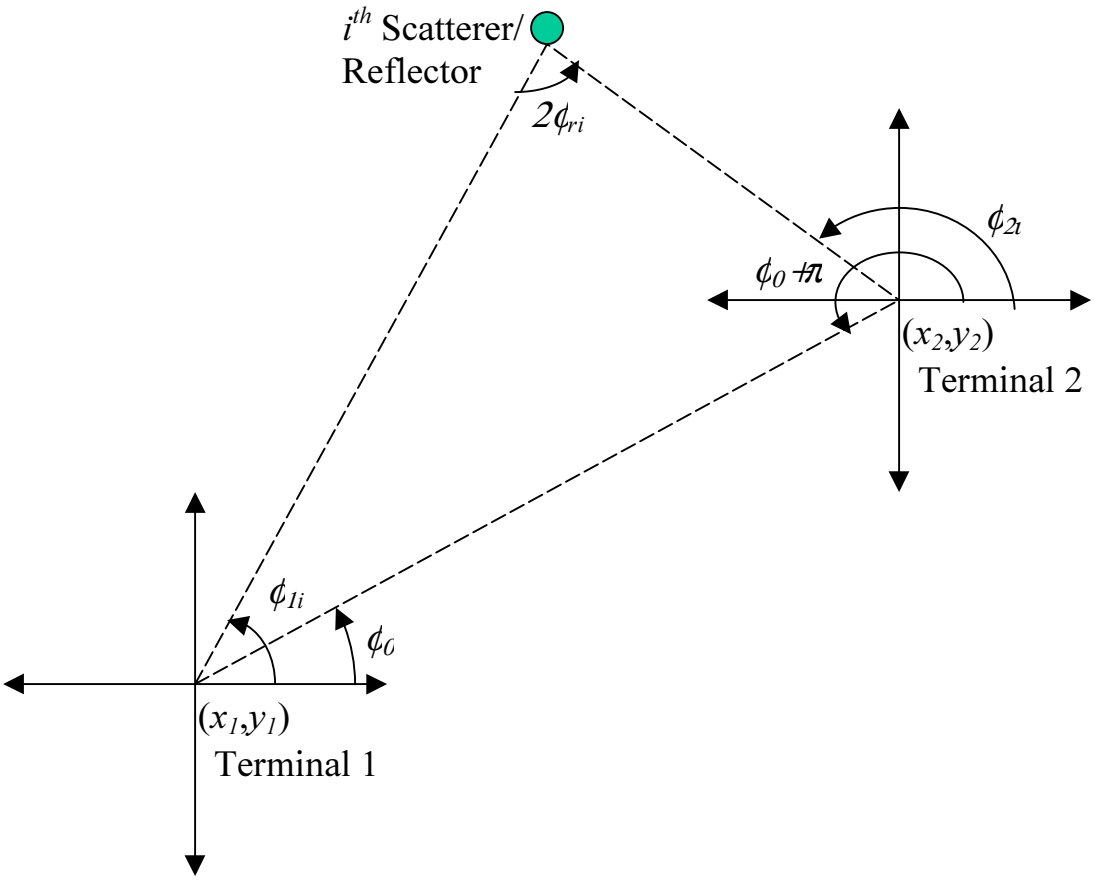

Figure 7-9. Geometry of link with multipath reflection for VMPS

The VMPS simulation software was implemented in MATLAB. Table 7-1 lists the m-files used, excluding the user interface, by function. The m-files are described in table format in Appendix B.

Table 7-1. List of m-files for polarization-sensitive propagation modeling (VMPS)

Functional Area:	General Propagation	Scatterer Distribu-tions	Array and Element Patterns	Reading, Writing, and Displaying Patterns	Pattern Rotation, Resampling, and Repolarization
m-files:	spsig.m getazpat.m reflect.m frescoeff.m aoadist.m	leescat.m	ap.m iso.m sdipole.m halfwave.m dirant.m gain.m	rcpat.m wcpat.m phipat.m thetapat.m threepat.m	rotpatvh.m rotate2.m resample.m polarize.m

Figure 7-10 shows the main user interface screen of the VMPS simulator. Spatial diversity is simulated by placing up to eight receiving antennas at any location within the propagation environment. The antenna patterns for each element can be entered individually to determine the polarization of the element and the angle response. For diversity performance, only one transmitter should be active and the transmitter, receiver, or both can be given a direction and speed of motion.

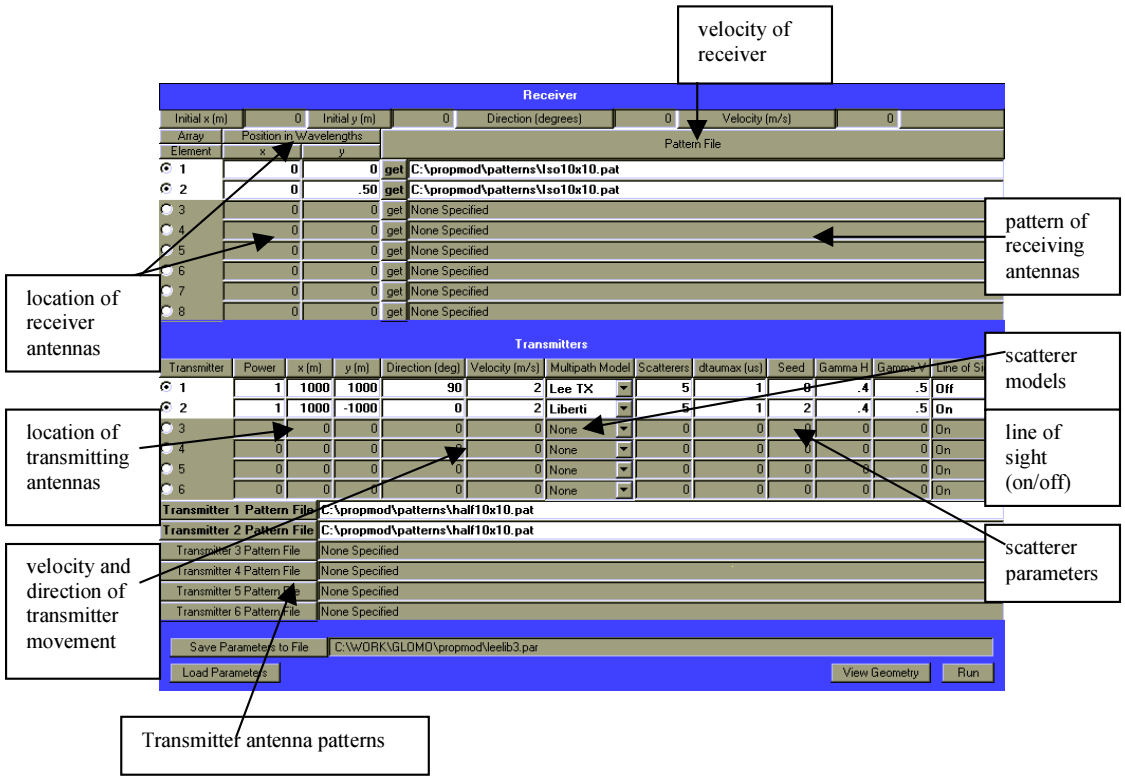

Figure 7-10. Main screen of VMPS user interface

The VMPS simulator can be used to simulate any of the diversity combining techniques discussed in Section 3.7 as well as adaptive beamforming algorithms. The following example uses maximal ratio combining on a two-branch diversity receiver.

7.5.3 Example: diversity combining in a non line-of-sight multipath channel

Figure 7-11 shows an example of a physical channel configuration simulated by VMPS. The transmitter (represented by a square) is moving at a speed of 2 m/s to the right with the receiver (represented by a circle) stationary. The receiver uses an array composed of two omnidirectional antennas separated by half a wavelength. The scatterer locations were randomly generated using Liberti's model (see Section 7.2.3) and their locations are denoted by the '+' symbol.

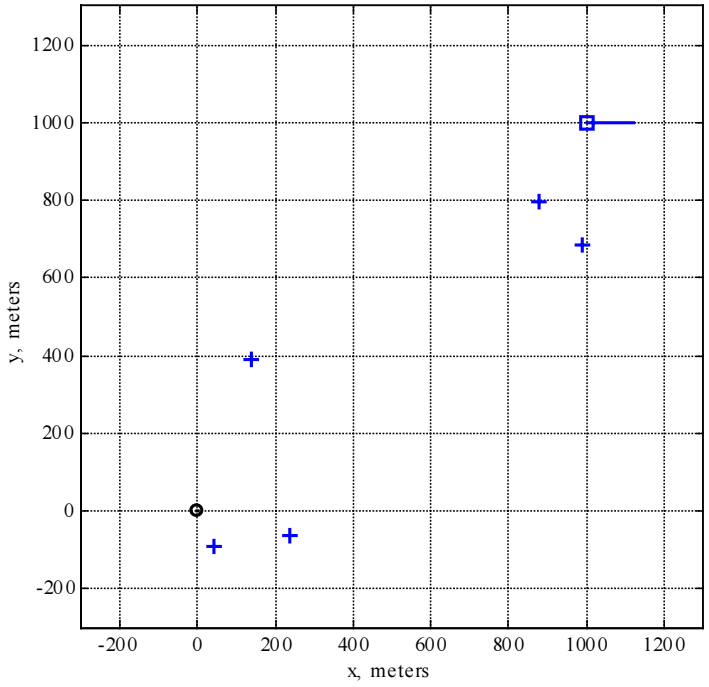

Figure 7-11. Diversity Simulation, location of transmitter, receiver, and scatterers

The signals at the two receiver branches were combined using maximal ratio combining (discussed in Ch. 3). Figure 7-12 illustrates the signal envelopes at both receiver elements as the transmitter moves over a distance of 4 meters (or a period of 2 seconds). The deep fades in signal amplitude are caused by the destructive interference of all the multipath components arriving at the receiving antennas. During some instances one of the antenna elements might be in a fade while the other might have a strong enough signal to produce an acceptably high signal at the receiver. A measure on how the signals fades on two antennas are related is given by the envelope cross-

correlation which typically varies from 0 (independent fading) to 1 (both signals fade at the same time), although small negative correlations are sometimes observed. The solid line on Figure 7-12 is the maximal ratio combination of both signals while the dashed lines are the signals received at both antennas. From the figure, one can observe that after combining the depth of the signal fades have been reduced significantly, in some cases by as much as 18 dB.

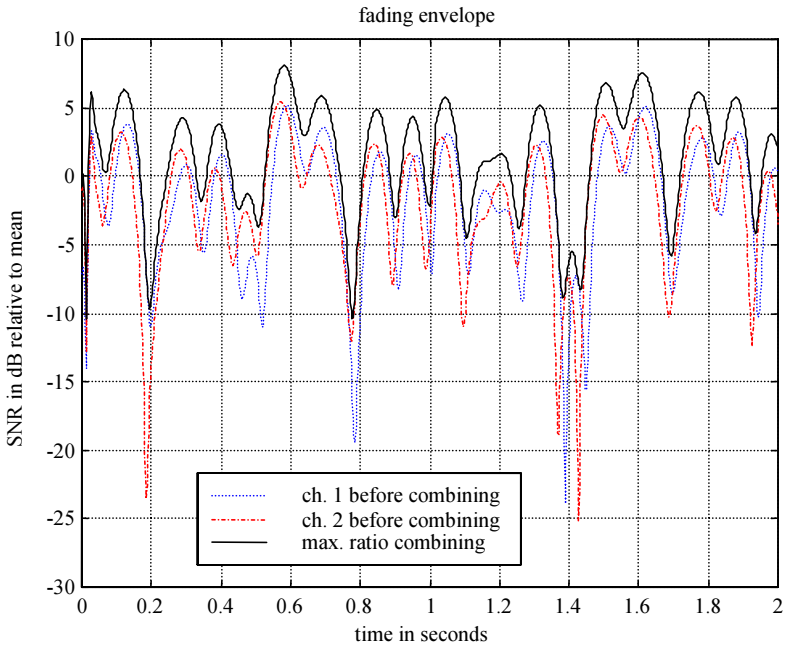

Figure 7-12. Fading envelopes of the signals before and after maximal ratio combining

The envelope correlation for this simulation was found to be 0.73, this means that both signals are strongly correlated and the signal fades occurr at about the same time in both branches. The diversity gain, using maximal ratio combining, can be measured from the cumulative distribution function as shown in Figure 7-13. The 10% diversity gain represents the level that the 90% reliability point is increased by after combining when compared to the branch with the strongest power. The 90% reliability level is the value a signal exceeds for 90% of the time, which translates to the 10% cumulative probability value. From Figure 7-13, the diversity gain represents the horizontal difference between the combined signal and the branch with the largest signal power. A diversity gain of

8.32 dB and 4.31 dB was recorded for the 1% and 10% levels respectively from the graph.

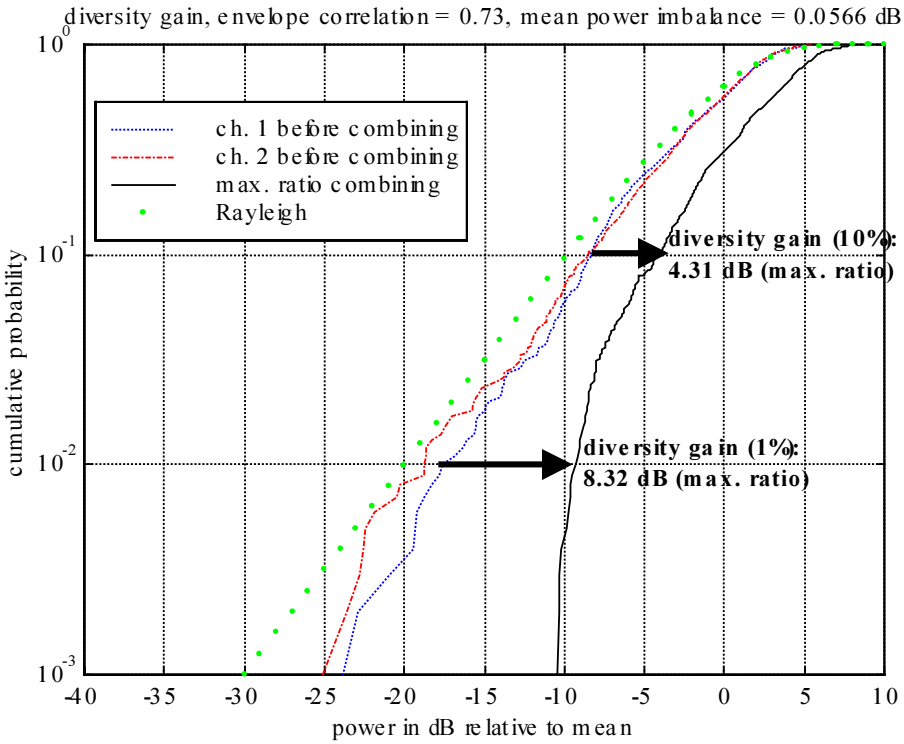

Figure 7-13. Cumulative probability distribution and diversity gain.

7.6 Conclusion

This chapter presented an overview of polarization-sensitive multipath propagation modeling. First, existing vector multipath propagation models were described. Second, reflection of polarized waves was discussed. This can be used to extend the existing vector channel models, which do not consider polarization. Then, a framework for polarization-sensitive propagation modeling was described that included coordinate systems, representation of antenna patterns with full polarization information, rotation of antenna patterns, gain of an arbitrarily polarized antenna, and polarization in multipath channels. Finally, the vector multipath propagation simulator (VMPS), a polarization-sensitive multipath propagation simulation software package, was described, including an example that used VMPS to evaluate diversity gain in a non line-of-sight multipath environment

References

[7.1] R. B. Ertel, et al., "Overview of Spatial Channel Models for Antenna Array Communication Systems," *IEEE Personal Communications*, pp. 10-22, February 1998.

[7.2] S. Y. Seidel and T. S. Rappaport, "Site-specific propagation prediction for wireless in-building personal communication system design," *IEEE Transactions on Vehicular Technology*, vol.43, no.4, Nov. 1994, pp.879-91.

[7.3] W. C. Y. Lee, *Mobile Communications Engineering*, McGraw Hill, New York, 1982.

[7.4] P. Petrus, J. H. Reed, and T. S. Rappaport, "Geometrically Based Statistical Channel Model for Macrocellular Mobile Environments," *IEEE GLOBECOM*, Vol. 2, pp. 1197-1201, 1996.

[7.5] J. C. Liberti and T. S. Rappaport, "A Geometrically Based Model for Line-of-Sight Multipath Radio Channels," *IEEE Vehicular Technology Conference*, Vol. 2, pp. 844-848, 1996.

[7.6] C. A. Balanis, *Advanced Engineering Electromagnetics*, John Wiley & Sons, 1989.

[7.7] J. C. Liberti, "Antenna File Formats for SISP," Draft Report for MPRG, Virginia Tech, September 6, 1994.

[7.8] A. C. Ludwig, "The Definition of Cross Polarization," *IEEE Transactions on Antennas and Propagation*, Vol. AP-21, pp. 116-119, Jan. 1973

[7.9] W. L. Stutzman and G. A. Thiele, *Antenna Theory and Design*, John Wiley & Sons, New York, 1981.

[7.10] W. L. Stutzman, Polarization in Electromagnetic Systems, Artech House, Norwood, MA, 1993.

[7.11] Kai Dietze, Carl Dietrich, and Warren Stutzman, *Vector Multipath Propagation Simulator (VMPS)*, Draft report, Virginia Tech Antenna Group, April 7, 1999.